JOURNAL OF THERMOPHYSICS AND HEAT TRANSFER
Vol. 23, No. 1, January–March 2009

Technical Notes

TECHNICAL NOTES are short manuscripts describing new developments or important results of a preliminary nature. These Notes should not exceed 2500 words (where a figure or table counts as 200 words). Following informal review by the Editors, they may be published within a few months of the date of receipt. Style requirements are the same as for regular contributions (see inside back cover).

Advancement in Numerical Study of Gas Flow and Heat Transfer in Microscale

Shidvash Vakilipour* and Masoud Darbandi†
Sharif University of Technology,
11365 Tehran, Iran

DOI: 10.2514/1.37037

I. Introduction

THE fast progress in micro/nanoscales has drawn the attention of many numerical workers to extend suitable numerical approaches to analyze micro/nanoflows more accurately. One important challenge has been in simulating gas flow and heat transfer in long microchannels [1]. Indeed, the flow and heat behaviors in micro/nanochannels differ from those in minichannels. For example, Pfahler et al. [2] conducted some experiments in microchannels with $Kn = 0.088$ and 0.04, measured the friction factor of flow, and concluded that the magnitude of (fRe) would be less than that in miniscale channels. This conclusion was later shown by the numerical investigators, for example, see [1,3]. Shih et al. [4] carried out some experiments to measure the mass flow rate and axial pressure in long microchannels under isothermal conditions considering $Kn_{\text{out}} = 0.16$ and 0.055. They reported higher nonlinearities in mass flow rate and axial pressure distribution as the inlet-to-outlet pressure ratio increased. Kavehpour et al. [5] imposed the first-order slip velocity and temperature jump boundary conditions to model flow and heat in a long microchannel with $L/H = 8000$. They examined both isothermal ($Kn_{\text{out}} \leq 0.165$) and constant heat flux ($Kn_{\text{out}} \leq 0.1$) wall boundary conditions. They illustrated that an increase in the Knudsen number would decrease the Nusselt number. Beskok and Karniadakis [6] employed a proposed high-order slip velocity boundary condition to solve isothermal flow in a channel covering a wide range of Knudsen numbers. They employed a variable fluid viscosity along the channel to adjust the correct mass flow rate.

Literature shows that the past experimental, theoretical, and continuum-based numerical efforts have mostly studied heat transfer in microchannels where $Kn \leq 0.15$. Evidently, the heat transfer behaviors in transition and free-molecular flow regimes ($Kn > 0.1$) differ from those in the slip-flow regime. On the other hand, the continuum-based methods associated with the first-order slip velocity and temperature jump boundary conditions are not suitable to treat flows with Knudsen numbers above 0.1. Alternatively, the molecular-based methods, for example, direct simulation Monte Carlo (DSMC), provide reliable approaches to study flow and heat transfer from free-molecular to slip-flow regimes. However, these methods have been used to simulate flow and heat transfer in relatively short channels. This is because the simulation of flow in long microchannels is computationally expensive for the molecular-based methods. Karniadakis et al. [1] provide more details in limitations and errors that occurred in using DSMC. Therefore, there is a lack of investigation to treat the heat transfer in early transition regimes ($0.1 < Kn < 1$) in long micro- to nanoscale channels using either continuum-based or molecular-based methods. The current authors have already developed a finite volume method and simulated flow in the entrance region of relatively short microchannels [7]. We further extended our preliminary work and developed an inlet thermal boundary condition to investigate the rarefaction effects on the flow behavior in the hydraulically and thermally developing zones in short microchannels where $0 \leq Kn \leq 0.5$. We applied high-order slip velocity and temperature jump boundary conditions to solve high Knudsen number regimes [8].

In this work, we further study the gas flow and heat transfer in a long microscale channel with $L/H = 8000$. We apply a second-order slip velocity boundary condition to handle flow in the early transition regime. Contrary to past investigations, we expand our study to impose constant heat flux boundary condition at the wall. The present results are evaluated against available theoretical solutions and experimental data. We will also present the effects of thermal rarefaction on the pressure and Knudsen number distributions along the channel.

II. Boundary Condition Treatments

The detail of numerical modeling is very long, see [9–11]. In this section, we briefly describe the ways that the second-order slip velocity and temperature jump boundary conditions are imposed at the solid walls of a microchannel conducting rarefied gas flow. As is known, the flow status becomes transitional as the Knudsen layer thickness increases to more than one-tenth of the bulk flow size. Typically, the first-order boundary conditions cease to be accurate above $Kn > 0.1$, see [12]. Piekos and Breuer [13] also showed that the Maxwell slip boundary condition would fail above around $Kn = 0.15$. In other words, the first-order slip velocity and temperature jump boundary conditions do not work accurately in the early transition regime and produce erroneous solutions. To overcome these shortcomings, we use the second-order slip velocity and temperature jump boundary conditions, which are derived using a gas–surface interface mechanism. Karniadakis et al. [1] showed that the second-order accurate mean tangential (slip) velocity of gas molecules on the wall can be calculated from

$$u_s^* = [u_\lambda^* + (1 - \sigma_v)u_\lambda^* + \sigma_v u_w^*]/2 \tag{1}$$

where σ_v is the tangential accommodation coefficient, $*$ denotes dimensionless variables, that is, $u^* = u/u_{\text{in}}$, and the subscripts in, w, and λ denote inlet, wall, and one mean-free path length from the wall, respectively. Contrary to the first-order Maxwell slip boundary condition [7], Eq. (1) is free from any velocity gradient calculations and provides relatively less computational efforts.

Received 7 February 2008; revision received 21 July 2008; accepted for publication 26 July 2008.

*Ph.D., Research Fellow, Department of Aerospace Engineering, Post Office Box 11365-8639; vakili@mehr.sharif.edu.

†Professor, Department of Aerospace Engineering, Post Office Box 11365-8639; darbandi@sharif.edu (Corresponding Author).

Karniadakis et al. [1] used Taylor series expansion and derived a high-order temperature jump boundary condition. Its nondimensional form is given by

$$T_s^* = (CT_\lambda^* + T_w^*)/(1 + C)$$
$$C = 2\gamma(2 - \sigma_T)/[\sigma_T(\gamma + 1)Pr] \tag{2}$$

where the thermal accommodation coefficient σ_T denotes the exchange ratio of energy flux between the wall and the fluid particles. The Prandtl number and gas specific heat ratio are shown by Pr and γ, respectively.

Equation (1) is used to calculate the slip velocity u_s^* considering the knowledge of u_λ^* and u_w^* velocity magnitudes. However, the thermal boundary condition given by Eq. (2) is applied differently for the constant wall and constant heat flux boundary conditions. In the former case, the temperature of the surface located on the solid wall T_s^* is unknown, and it should be calculated using the temperature at one mean-free-path away from the wall T_λ^* and the wall temperature T_w^*. However, the wall temperature T_w^* is unknown in the latter case, and it should be calculated using the temperature of the surface located on the solid wall T_s^* and the temperature at one mean-free-path away from the wall T_λ^*. We apply constant wall heat flux boundary condition in this work; hence, the wall temperature is calculated from Eq. (2).

We study the flow in a microscale channel with $L/H = 8000$. The channel is long enough to compare our results with those of [3]. Because the geometry and boundary conditions are symmetric, only one-half of the channel is simulated here. The inlet is discretized to 19 nodes and they are clustered near the wall. The longitudinal dimension is discretized to 1500 divisions using a nonuniform grid distribution, in which the ratios of the first and last cell lengths to the channel height are 0.01 and about 5.33, respectively. The inlet boundary condition is applied at the inlet of the channel, considering a uniform axial velocity of $u^* = 1$ and a transversal velocity of $v^* = 0$. Symmetric boundary conditions are applied at the channel centerline. Using the magnitude of the inlet Mach number, a uniform pressure distribution of $P_{\text{out}} = p_{\text{out}}/[(\gamma - 1)M_{\text{in}}^2]$ is specified at the outlet boundary. Additionally, the convection and diffusion fluxes are conserved at the outlet boundary [14]. The Prandtl, Reynolds, and inlet Mach numbers are 0.71, 0.075, and 0.002, respectively.

III. Results and Discussion

There are some theoretical, experimental, and continuum-based numerical investigations which study heat transfer in the slip-flow regime in microscale channels. However, there is no major numerical work, either continuum-based or molecular-based, to treat the momentum and heat transfer in long channels performing transition flow regime status. Therefore, our comparisons are limited to slip-flow regime. At the first stage, we test compressible isothermal flow taken from [6]. Figure 1 shows the velocity profiles at four sections, where their Knudsen numbers are 0.05, 0.2, 0.35, and 0.5. Our experience [7] shows that the fully developed conditions are achieved before $x^* = x/H = 1.5$ if the flow is incompressible and $Re \leq 1.0$. However, the velocity profiles do not reach to a limiting shape in compressible flow. The current velocity profiles are compared with those of high-order analytical solutions. There are excellent agreements between them, indicating that the current velocity profiles perform second-order accuracy, as was predicted in Sec. II.

We also evaluate the extended boundary conditions in simulating helium flow through microchannels and compare our pressure distributions with those of [4]. The helium properties are calculated at the atmospheric condition. Figure 2 illustrates the axial gauge pressure distributions along the channel centerline. Following [4], the current results were obtained at $P_{\text{in}} = 8.7$, 12.8, 13.6, and 19.0 psig (i.e., $P_{\text{in}} = 60.0$, 88.3, 93.8, and 131.0 kPa gauge). The outlet Knudsen number is 0.16. As is seen, the pressure distributions perform higher nonlinearity as the inlet-to-outlet pressure ratio increases. This is because the compressibility effects dominate the rarefaction effects at higher pressure ratios, and vice versa. The present results are in good agreement with the experimental data.

At the second stage, we study the rarefied gaseous flow in transition regime under uniform heat flux boundary conditions. As was mentioned before, this study has not been carried out by either continuum-based or molecular-based methods. In this case, the outlet Knudsen is $Kn_{\text{out}} = 0.5$. The dimensionless wall heat flux ($q'' = \partial T^*/\partial x^*$) is constant along the channel wall and its value is $q'' = 5 \times 10^{-5}, 1 \times 10^{-4}, 2 \times 10^{-4}, 4 \times 10^{-4}$, and 8×10^{-4}, whereas the outlet pressure is identical for all four cases. Figure 3 illustrates the deviation of axial pressure distributions from the corresponding linear pressure drop along the heated channel for an incompressible flow case. The dashed lines stand for the isotherm analytical solutions, which are derived by imposing an inlet-to-outlet pressure ratio equal to those prescribed in constant heat flux cases [1], that is, $P_{\text{in}}/P_{\text{out}} = 18.0$, 15.5, 14.0, 13.2, and 12.7. Additionally, we

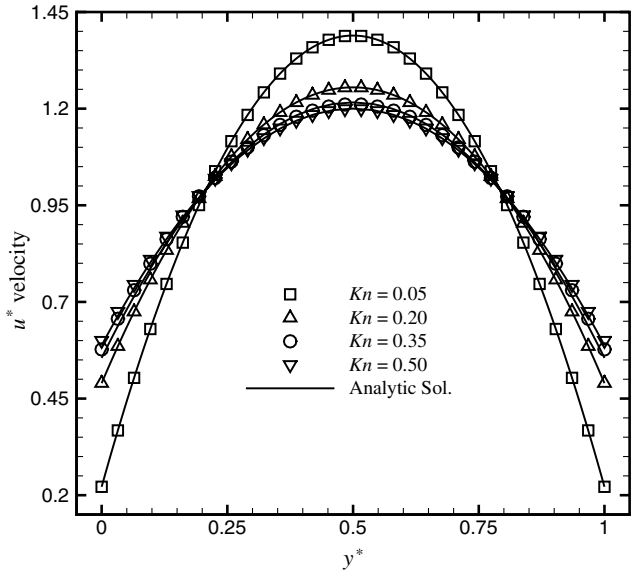

Fig. 1 Velocity profiles at four sections in the channel compared with analytical solutions [6].

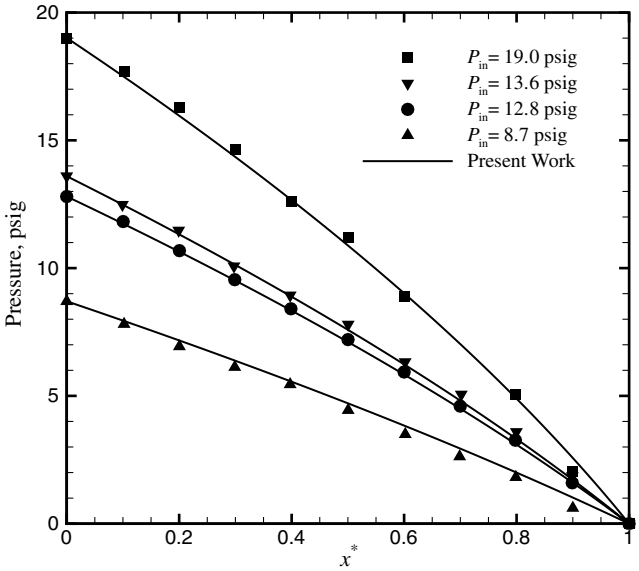

Fig. 2 Comparison of current pressure distributions with measurements [4] (symbols); the gauge pressure varies from 0 to 20 psig (i.e., 0–137.9 kPa gauge).

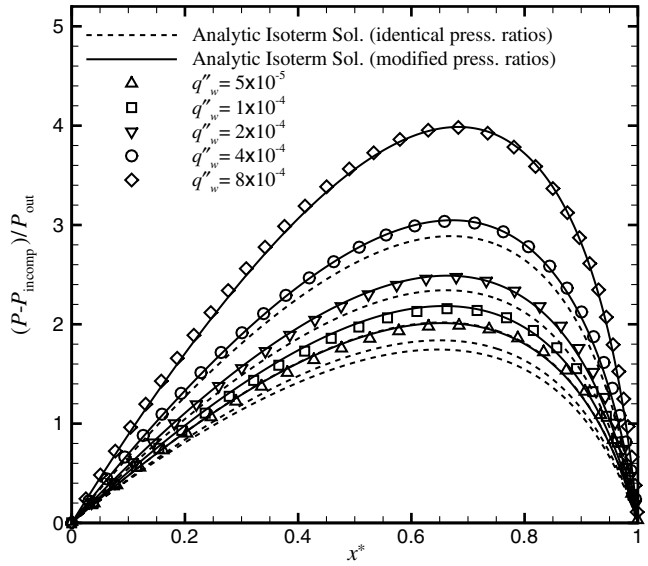

Fig. 3 Current pressure deviation from the linear incompressible pressure distribution and comparison with two types of isotherm analytical solutions [1].

obtained the isotherm analytical solutions using modified inlet-to-outlet pressure ratios. In the modified form, the analytical solutions fit the current constant heat flux results in the channel. The modified pressure ratios are $P_{in}/P_{out} = 22.8$, 18.7, 16.2, 14.8, and 14.0. As is seen, the pressure performs higher nonlinearity in constant heat flux cases than the isothermal one when identical inlet-to-outlet pressure ratios are imposed. On the other hand, the nonlinearities due to implementing the modified inlet-to-outlet pressure ratios are always higher than those of imposing identical pressure ratios. Also, as the wall heat flux increases, the nonlinearity in the pressure distribution becomes more augmented for both types of inlet-to-outlet pressure ratio implementation. This is evident because the density variation is higher at higher heat flux rates and, consequently, the compressibility effects become more pronounced in such conditions.

Figure 4 shows the Knudsen number distributions along the channel, imposing various wall heat flux rates. The current results are compared with that of an adiabatic channel. It should be noted that the inlet Knudsen number is 0.05 and the inlet Mach number and the outlet pressure are identical for all adiabatic and nonadiabatic cases.

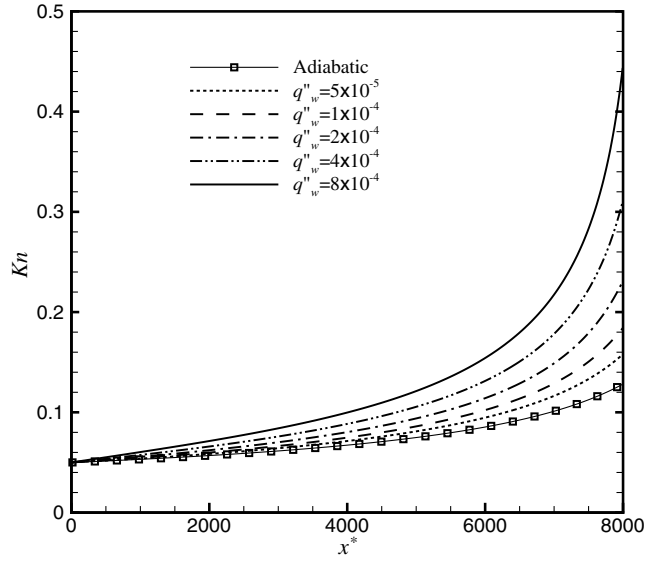

Fig. 4 Knudsen number distribution in the channel imposed by different wall heat flux rates.

Although the flow at the inlet is in the slip-flow regime, it undergoes a transition regime close to the outlet. The Knudsen number distributions obviously show that the rarefaction becomes significant as the heat rate to flow increases. Additionally, the rate of compressibility (Mach number) variation increases as the heat rate increases. The figure also shows that the rate of rarefaction (Knudsen number) increases as the flow is heated more. The increase is more rapid in higher heat flux rates.

IV. Conclusions

The flow and heat transfer were investigated in a long microscale channel imposing the second-order slip velocity and temperature jump boundary conditions at the channel walls. The current results were evaluated against reliable analytical solutions and available experimental data. Our velocity profiles performed second-order accuracy and our pressure distributions agreed well with the available experimental data. We evaluated the compressibility effects for various inlet-to-outlet pressure ratios. It was shown that the early transition flow conditions would start at different longitudinal locations when the heat flux rate into the channel was changed. A higher heat flux rate would result in a faster early transition regime condition, indicating that the flow is mostly in the transition regime. On the other hand, the flow in micro- and nanoscale channels with constant heat flux boundary conditions differs from that of a channel with constant wall temperature. The differences become more augmented as the rate of heat flux increases. This work indicates that robust continuum-based numerical methods can be safely used to study the gas flow and heat transfer in microscales.

References

[1] Karniadakis, G. E., Beskok, A., and Aluru, N., *Microflows and Nanoflows: Fundamentals and Simulation*, Springer–Verlag, New York, 2005.

[2] Pfahler, J., Harley, J., Bau, H., and Zemel, J. N., "Gas and Liquid Flow in Small Channels," *Proceedings of ASME Winter Annual Meeting, Micromechanical Sensors Actuator Systems*, DSC32, American Society of Mechanical Engineers, Fairfield, NJ, 1991, pp. 49–60.

[3] Beskok, A., and Karniadakis, G. E., "Simulation of Heat and Momentum Transfer in Complex Microgeometries," *Journal of Thermophysics and Heat Transfer*, Vol. 8, No. 4, 1994, pp. 647–655. doi:10.2514/3.594

[4] Shih, J. C., Ho, C., Liu, J., and Tai, Y., "Monatomic and Polyatomic Gas Flow Through Uniform Microchannels," *American Society of Mechanical Engineers: Microelectromechanical Systems Division* DSC59, American Society of Mechanical Engineers, Fairfield, NJ, 1996, pp. 197–203.

[5] Kavehpour, H. P., Faghri, M., and Asako, Y., "Effects of Compressibility and Rarefaction on Gaseous Flows in Microchannels," *Numerical Heat Transfer, Part A: Applications*, Vol. 32, No. 7, 1997, pp. 677–696. doi:10.1080/10407789708913912

[6] Beskok, A., and Karniadakis, G. E., "A Model for Flows in Channels, Pipes, and Ducts at Micro and Nano Scales," *Microscale Thermophysical Engineering*, Vol. 3, No. 1, 1999, pp. 43–77. doi:10.1080/108939599199864

[7] Darbandi, M., and Vakilipour, S., "Developing Consistent Inlet Boundary Conditions to Study the Entrance Zone in Microchannels," *Journal of Thermophysics and Heat Transfer*, Vol. 21, No. 3, 2007, pp. 596–607. doi:10.2514/1.27509

[8] Darbandi, M., and Vakilipour, S., "Developing Consistent Inlet Thermal Boundary Condition in Micro/Nano Scale Channels with Heat Transfer," *The ASME International Conference in Micro/Nanoscale Heat Transfer*, American Society of Mechanical Engineers, Fairfield, NJ, 2008, p. 10.

[9] Darbandi, M., and Schneider, G. E., "Analogy-Based Method for Solving Compressible and Incompressible Flows," *Journal of Thermophysics and Heat Transfer*, Vol. 12, No. 2, 1998, pp. 239–247. doi:10.2514/2.6327

[10] Darbandi, M., Schneider, G. E., "Application of an All-Speed Flow

Algorithm to Heat Transfer Problems," *Numerical Heat Transfer, Part A: Applications*, Vol. 35, No. 7, 1999, pp. 695–715. doi:10.1080/104077899274985

[11] Darbandi, M., and Vakilipour, S., "Developing Implicit Pressure-Weighted Upwinding Scheme to Calculate Steady and Unsteady Flows on Unstructured Grids," *International Journal for Numerical Methods in Fluids*, Vol. 56, No. 2, 2008, pp. 115–141. doi:10.1002/fld.1451

[12] Gad-el-Hak, M., "The Fluid Mechanics of Microdevices: The Freeman Scholar Lecture," *Journal of Fluids Engineering*, Vol. 121, March 1999, pp. 5–33. doi:10.1115/1.2822013

[13] Piekos, E. S., and Breuer, K., "DSMS Modeling of Micromechanical Devices," *30th Thermophysics Conference*, AIAA Paper 95-2089, June 1995.

[14] Darbandi, M., and Vakilipour, S., "Using Fully Implicit Conservative Statements to Close Open Boundaries Passing Through Recirculations," *International Journal for Numerical Methods in Fluids*, Vol. 53, No. 3, 2007, pp. 371–389. doi:10.1002/fld.1283